arXiv:1703.09589v1 [math.NA] 28 Mar 2017

NUMERICAL ALGORITHM FOR C^2-SPLINES ON SYMMETRIC SPACES

GEIR BOGFJELLMO[1], KLAS MODIN[1], AND OLIVIER VERDIER[2]

Abstract. Cubic spline interpolation on Euclidean space is a standard topic in numerical analysis, with countless applications in science and technology. In several emerging fields, for example computer vision and quantum control, there is a growing need for spline interpolation on curved, non-Euclidean space. The generalization of cubic splines to manifolds is not self-evident, with several distinct approaches. One possibility is to mimic the acceleration minimizing property, which leads to *Riemannian cubics*. This, however, require the solution of a coupled set of non-linear boundary value problems that cannot be integrated explicitly, even if formulae for geodesics are available. Another possibility is to mimic De Casteljau's algorithm, which leads to *generalized Bézier curves*. To construct C^2-splines from such curves is a complicated non-linear problem, until now lacking numerical methods. Here we provide an iterative algorithm for C^2-splines on Riemannian symmetric spaces, and we prove convergence of linear order. In terms of numerical tractability and computational efficiency, the new method surpasses those based on Riemannian cubics. Each iteration is parallel, thus suitable for multi-core implementation. We demonstrate the algorithm for three geometries of interest: the n-sphere, complex projective space, and the real Grassmannian.

MSC-2010: 41A15, 65D07, 65D05, 53C35, 53B20, 14M17

Keywords: De Casteljau, cubic spline, Riemannian symmetric space, Bézier curve

Contents

1. Introduction 2
2. Generalized Bézier curves on symmetric spaces 3
3. Numerical algorithm 7
4. Examples 9
5. Outlook 12
Appendix A. Identities and bounds on symmetric spaces 14
Appendix B. C^2 continuity 17
Appendix C. Convergence of the fixed-point method 18
Appendix D. Python implementation 25
References 25

[1]Mathematical Sciences, Chalmers and University of Gothenburg, Sweden
[2]Department of Computing, Mathematics and Physics, Western Norway University of Applied Sciences, Bergen, Norway
E-mail addresses: geir.bogfjellmo@chalmers.se, klas.modin@chalmers.se, olivier.verdier@hvl.no.
Date: 2017-03-29.

1. Introduction

We address the following.

Problem 1. Given a set of point $\{ p_i \}_{i=0}^N$ on a connected manifold M, construct a C^2 path $\gamma\colon [0, N] \to M$ such that $\gamma(i) = p_i$.

For $M = \mathbb{R}^n$ every textbook in numerical analysis teaches *cubic splines*, i.e., piecewise polynomials of order 3 with matching first and second derivatives. However, the generalization of cubic splines to curved space is non-trivial, essentially because polynomials are not well-defined on manifolds. Interpolating paths on manifolds are, nevertheless, needed in a growing number of applications. In the realization of quantum computers, for example, quantum control of qubits leads to an interpolation problem in complex projective space $\mathbb{C}P^n$ (see § 4.2). In computer vision, as another example, the recognition of a point cloud up to affine transformations is naturally identified with an element in the Grassmannian $\mathrm{Gr}(k, n)$ (see § 4.3).

If M is a Riemannian manifold, a natural generalization of cubic splines are *Riemannian cubics* [12, 2]. They are based on minimizing acceleration under interpolation constraints, by solving the problem

$$\min_{\gamma(i)=p_i} \int_0^N |\nabla_{\dot\gamma(t)}\dot\gamma(t)|^2 \,\mathrm{d}t. \tag{1}$$

The corresponding Euler–Lagrange equation is a fourth order ODE on M with complicated, coupled boundary conditions [12]. In addition to the Euclidean case, explicit solutions to the initial-value problem are known for so called *null Lie quadratics* on $\mathrm{SO}(3)$ and $\mathrm{SO}(2, 1)$ equipped with the bi-invariant Riemannian metric [11]. For other cases, even when geodesics are explicitly known, one is left with numerical ODE methods, combined, for example, with a shooting method to match the boundary conditions. This approach is computationally costly and the associated convergence analysis is involved. Another possibility is to only approximatelly fulfill the interpolation constraints by incorporating them in the minimization functional and then use a steepest-descent method on the space of curves [15]. Also this approach is costly.

If M is a manifold for which the geodesic boundary problem can be solved explicitly, there is a natural concept of *generalized Bézier curves* (GBC). They are based on a direct generalization of De Casteljau's algorithm [13]. Splines can then be constructed by gluing piecewise GBC with matching boundary conditions. In this way, a fully explicit algorithm for C^1-splines on Grassmannian and Stiefel manifolds has been developed [8]. The C^2-condition, however, first derived by Popiel and Noakes [14], is significantly more complicated than the C^1-condition. For this reason, there is a lack of numerical algorithms for C^2-splines. Nevertheless, C^2 continuity is often required in applications, to avoid discontinuities in accelerations.

In this paper we give the first numerical algorithm for C^2-splines based on GBC. Instead of treating all Riemannian manifolds, we focus on the subclass of *symmetric spaces* (see § 2.1). Such manifolds are of high interest in applications, and include, e.g., spheres, hyperbolic space, real and complex projective spaces, and Grassmannian manifolds (see Table 1). In many cases, the geodesic boundary value problem on a symmetric space has explicit solution (a prerequisite for De Casteljau's algorithm). The

	M	G	H	Implementation
Euclidean space	$\mathbb{R}^n$	$\mathrm{SE}(n)$	$\mathrm{SO}(n)$	`Flat`
n-sphere	S^n	$\mathrm{O}(n+1)$	$\mathrm{O}(n)$	`Sphere`
Hyperbolic space	H^n	$\mathrm{O}(n,1)$	$\mathrm{O}(n)$	`Hyperbolic`
Real Grassmannian	$\mathrm{Gr}(k,n)$	$\mathrm{O}(n)$	$\mathrm{O}(k)\times\mathrm{O}(n-k)$	`Grassmannian`
Orthogonal group	$\mathrm{O}(n)$	$\mathrm{O}(n)\times\mathrm{O}(n)$	$\mathrm{O}(n)$	
Complex projective space	$\mathbb{C}P^n$	$\mathrm{U}(n+1)$	$\mathrm{U}(n)\times\mathrm{U}(1)$	`Projective`
Complex Grassmannian	$\mathrm{Gr}_{\mathbb{C}}(k,n)$	$\mathrm{U}(n)$	$\mathrm{U}(k)\times\mathrm{U}(n-k)$	
Unitary group	$\mathrm{U}(n)$	$\mathrm{U}(n)\times\mathrm{U}(n)$	$\mathrm{U}(n)$	
Co-variance matrices	$P(n)$	$\mathrm{GL}(n)$	$\mathrm{O}(n)$	

TABLE 1. Some examples of Riemannian symmetric spaces. For the details of the corresponding symmetric space decomposition, see [10, § 5]. In the right-most column, we give the geometry class to use when interpolating with our `Python` package; we refer to Appendix D for example usage.

original C^2-condition of Popiel and Noakes, however, is still complicated. We now list the specific contributions of our paper.

(1) Using the special homogeneous space structure of symmetric spaces, we give a significant simplification of the C^2-condition (Theorem 2.2).
(2) Using the new C^2-condition, we construct an algorithm based on fixed-point iterations (Algorithm 1).
(3) We prove convergence of the algorithm under conditions on the maximal distance between consecutive interpolation points (Theorem 3.1).

The paper is organized as follows. In § 2 we first give a brief description of Riemannian symmetric spaces and thereafter describe the construction of generalized Bézier curves. We also formulate the C^2-condition. In § 3 we give the numerical algorithm and we formulate the convergence result. Numerical examples are given in § 4. An outlook towards future work is given in § 5. The proofs of the C^2-condition and the convergence result are long and technical, and therefore given in Appendix A-C. In Appendix D we give a brief demonstration of an easy-to-use open-source `Python` package implementing our interpolation algorithm for several geometries.

2. Generalized Bézier curves on symmetric spaces

Let us describe the construction of generalized Bézier curves on a symmetric space. The construction relies on a notion of *interpolation* between two points on the manifold, generalizing the notion of a *geodesic* on a Riemannian manifold [9].

2.1. Symmetric spaces.

In this section we briefly recall symmetric spaces. A list of the most common examples of symmetric spaces is given in Table 1. For details, we refer to [16] or [4]. We assume that a Lie group G acts transitively on M, making M a *homogeneous space* [16, § 4]. We denote the action by

$$(g,p)\mapsto g\cdot p\in M. \tag{2}$$

For every point $p \in M$, we define the isotropy subgroup H_p at p

$$H_p \coloneqq \{\, g \in G \mid g \cdot p = p \,\}.$$

Now, the homogeneous space M is called a *symmetric space* if the Lie algebra $\mathfrak{g}$ of G has a direct sum decomposition

$$\mathfrak{g} = \mathfrak{h}_p \oplus \mathfrak{m}_p, \tag{3}$$

where $\mathfrak{h}_p$ is the Lie algebra of H_p, and the summands fulfill the following algebraic conditions

$$[\mathfrak{h}_p, \mathfrak{h}_p] \subset \mathfrak{h}_p, \qquad [\mathfrak{h}_p, \mathfrak{m}_p] \subset \mathfrak{m}_p, \qquad [\mathfrak{m}_p, \mathfrak{m}_p] \subset \mathfrak{h}_p. \tag{4}$$

If these conditions are satisfied at one point $p \in M$, then they are automatically valid at every point with

$$\mathfrak{h}_{g\cdot p} = \operatorname{Ad}_g \mathfrak{h}_p, \qquad \mathfrak{m}_{g\cdot p} = \operatorname{Ad}_g \mathfrak{m}_p$$

By differentiating the action map $(g, p) \mapsto g \cdot p$ with respect to the variables, we also obtain, on the one had, an *infinitesimal action* of $\mathfrak{g}$ on M, and, on the other hand, a *prolonged action* of G on TM. For $\xi \in \mathfrak{g}$ and $p \in M$, we denote the infinitesimal action by

$$(\xi, p) \mapsto \xi \cdot p \in T_pM. \tag{5}$$

For a fixed p, this map induces an isomorphism between $\mathfrak{m}_p$ and T_pM. The infinitesimal action (5) and the decomposition (3) thereby define a *principal connection* [10], i.e., a $\mathfrak{g}$-valued one-form ϖ on M which fulfills

$$\langle \varpi, v \rangle_p \cdot p = v \qquad \text{(consistency)} \tag{6a}$$

$$\langle \varpi, Tg \cdot v \rangle_{g\cdot p} = g \cdot \langle \varpi, v \rangle_p \qquad \text{(equivariance)} \tag{6b}$$

where the last action is the adjoint action of G on the Lie algebra $\mathfrak{g}$. By construction, $\mathfrak{m}_p = \varpi(T_pM)$.

Next, we define the *interpolating curve* $\eta\colon [0,1] \to M$ between two (nearby enough) points p_0 and p_1 as the unique curve satisfying

$$\eta(0) = p_0, \tag{7}$$

$$\eta(1) = p_1, \tag{8}$$

$$\frac{\mathrm{d}}{\mathrm{d}t} \langle \varpi, \eta'(t) \rangle = 0. \tag{9}$$

It follows that η is of the form

$$\eta(t) = \exp(t\xi) \cdot p_0 \tag{10}$$

with $\xi \in \mathfrak{m}_{p_0}$. Let us introduce the notation

$$[p_0, p_1]_t \coloneqq \eta(t).$$

In particular, notice that

$$[p_0, p_1]_0 = p_0, \tag{11}$$

$$[p_0, p_1]_1 = p_1. \tag{12}$$

In many (but not all) cases, a symmetric space M can be equipped with the structure of a Riemannian manifold, given through an H_p-invariant inner product $\langle \cdot, \cdot \rangle_p$ on $\mathfrak{m}_p$. In

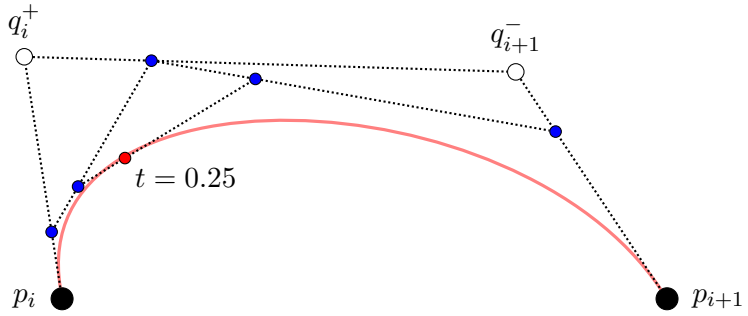

FIGURE 1. An illustration of the construction of a cubic Bézier curve using De Casteljau's algorithm at $t = 0.25$. The algorithm proceeds iteratively by choosing points at position 0.25 on each geodesic as indicated in the figure. The precise definition of the resulting curve is given in (13).

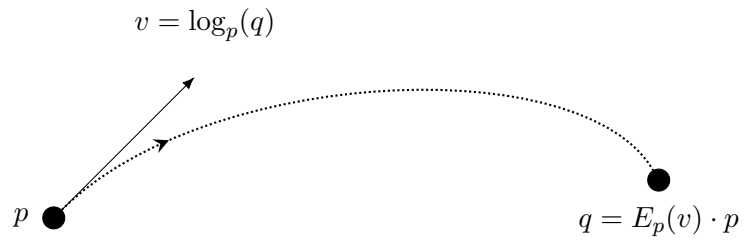

FIGURE 2. Illustration of the movement function E_p and of the logarithm described in § 2.3. The curve between p and q is a geodesic.

this case, the interpolating curves are geodesics. From here on, we shall assume that M is such a *Riemannian symmetric space*.

2.2. **De Casteljau's construction.** We briefly describe the De Casteljau construction, as illustrated on Figure 1. This algorithm constructs Bézier curves from interpolating curves. We focus on *cubic* Bézier curves. From four points p_0, q_0, q_1 and p_1, one defines the cubic Bézier curve $\gamma\colon [0,1] \to M$ by

$$\gamma(t) \coloneqq \Big[\big[[p_0, q_0]_t, [q_0, q_1]_t\big]_t, \big[[q_0, q_1]_t, [q_0, p_1]_t\big]_t\Big]_t. \tag{13}$$

Note that, by construction, $\gamma(0) = p_0$ and $\gamma(1) = p_1$.

2.3. **Exponential and logarithm on symmetric spaces.** For the formulation of the C^2 condition in § 2.4, and for the implementation of the algorithm, we need the following functions (see Figure 2).

(1) The action of a group element $g \in G$ on a point $x \in M$:

$$g \cdot x \in M \tag{14}$$

(2) A movement function E, which, to a point p and a velocity v at p, assigns an element $E_p(v) \in G$. This function should generate interpolating curves (9), i.e.,

it should be of the form

$$E_p(v) = \exp(\langle \varpi, v \rangle_p). \tag{15}$$

(3) The *logarithm*; given two points p and q in M, it is defined by

$$v \in T_pM, \qquad E_p(v) \cdot p = q, \qquad \Longleftrightarrow \qquad v = \log_p(q). \tag{16}$$

Throughout the paper we make the blanket assumption that p and q are never past conjugate points, so that the logarithm is always well-defined.

2.4. **Cubic splines and C^2 condition.** We shall now consider curves consisting of piecewise cubic Bézier curves. As we have seen in § 2.2, each cubic Bézier curve is determined by two interpolating points and two control points. To construct a curve of piecewise Bézier curves we therefore need to impose conditions on the control points (in addition to the interpolating conditions). On Euclidean space, the standard approach is to use the conditions for C^2 continuity at the interpolating points, which leads to a linear set of equations. On a general Riemannian manifold, the corresponding C^2 condition, given by Popiel and Noakes [14], is highly nonlinear, involving the inverse of the derivative of the Riemannian exponential. However, we now give a result that in the special case of symmetric spaces, the C^2 condition simplifies significantly, involving only the three operations (14), (15), and (16).

Definition 2.1. Let $\boldsymbol{p} = (p_0, \dots, p_N)$ be points on a symmetric space M. A *composite cubic Bézier curve* on M is a curve $\gamma\colon [0, N] \to M$ such that $\gamma(i) = p_i$ and the restriction $\gamma_i \coloneqq \gamma|_{[i,i+1]}$ is a cubic Bézier curve. The control points of γ_i are denoted q_i^+ and q_{i+1}^-. A C^2-continuous composite cubic Bézier curve is called a *cubic spline*.

The interpolating conditions ensure that γ is continuous (or C^0). However, for higher degree of continuity (C^1 or C^2), we need additional conditions on the control points. We now give such conditions.

Theorem 2.2. *Let M be a Riemannian symmetric space and let $\gamma\colon [0, N] \to M$ be a composite cubic Bézier curve. Consider the conditions on the control points given by*

$$\log_{p_i}(q_i^+) = -\log_{p_i}(q_i^-) =: v_i \tag{17}$$

$$\log_{p_i}(\exp(-\xi_i) \cdot q_{i+1}^-) - \log_{p_i}(q_i^+) = \log_{p_i}(\exp(\xi_i) \cdot q_{i-1}^+) - \log_{p_i}(q_i^-), \tag{18}$$

where $\xi_i = \langle \varpi, v_i \rangle_{p_i}$.

(1) If condition (17) is fulfilled, then γ is a C^1-curve.

(2) If conditions (17) and (18) are fulfilled, then γ is a C^2-curve, i.e., a cubic spline.

Furthermore, if γ fulfills the C^2-conditions (17) and (18), then it is uniquely determined either by clamped boundary conditions, where $\gamma'(0)$ and $\gamma'(N)$ are prescribed, or by natural boundary conditions, where $\nabla_{\gamma'(0)}\gamma'(0) = \nabla_{\gamma'(0)}\gamma'(0) = 0$.

Remark 2.3. Notice how (17) and (18) are generalizations of the first and second order finite differences in Euclidean geometry. Indeed, in this case condition (17) reads

$$q_i^+ - p_i = -(q_i^- - p_i) \tag{19}$$

and condition (18) reads

$$q_{i-i}^+ - 2q_i^- + p_i = q_{i+1}^- - 2q_i^+ + p_i. \tag{20}$$

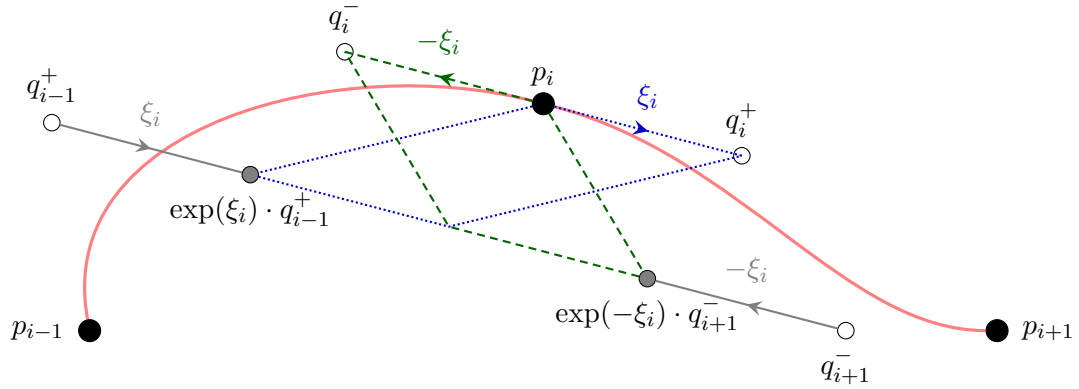

FIGURE 3. An illustration of the C^2-condition in Theorem 2.2. The sum of the two vectors at p_i generating the dashed green geodesics should equal the sum of the two vectors at p_i generating the dotted blue geodesics. Notice that the action of $\exp(\xi_i)$ on q_{i-1}^+ and q_{i+1}^- does not generate geodesics from these points, since ξ_i does not belong to $\mathfrak{m}_{q_{i-1}^+}$ or $\mathfrak{m}_{q_{i+1}^-}$. For this reason, the condition (18) in Theorem 2.2 does not work for arbitrary Riemannian manifolds.

See Figure 3 for a geometric illustration of the C^2-condition (18).

Outline of proof. The details of the proof are rather technical and therefore given in Appendix B. However, for convenience we also provide an outline of the proof:

(1) The C^2 condition in the case of Riemannian symmetric spaces is given by Popiel and Noakes [14, Sec. 4]. It is expressed in terms of the derivative of the *symmetry function* $I_p(q) = E_p(-\log_p(q))$.
(2) Using the special symmetric space structure, we show that the derivative of I_p can be expressed solely in terms of the movement function E_p (Lemma A.3).
(3) Together with a result on equivariance of the log function (Lemma A.4) we can then simplify the original Riemannian symmetric space C^2 condition by Popiel and Noakes [14] to the one given by (18).

□

3. NUMERICAL ALGORITHM

We shall now construct a fixed point iteration algorithm for cubic splines on symmetric spaces, based on the C^2 condition in Theorem 2.2. To this end, we parameterize the control points q_i^- and q_i^+ by the corresponding tangent vectors v_i as defined in Theorem 2.2. Next, let

$$w_i(\xi_{i-1},\xi_i,\xi_{i+1}) = \log_{p_i}(\exp(-\xi_i)\exp(-\xi_{i+1})\cdot p_{i+1}) - \log_{p_i}(\exp(\xi_i)\exp(\xi_{i-1})\cdot p_{i-1}). \quad (21)$$

The iteration map over $\boldsymbol{v} \coloneqq (v_1,\dots,v_{N-1})$ is then given by

$$\boldsymbol{v} \mapsto \frac{1}{4}\boldsymbol{w}(\langle \varpi, \boldsymbol{v}\rangle) + \frac{1}{2}\boldsymbol{v}, \quad (22)$$

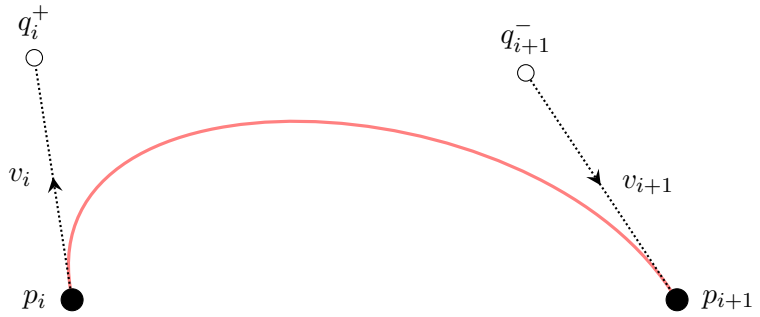

FIGURE 4. An illustration of the control points and the corresponding velocities. We define a velocity v_i at every point p_i. From that velocity, we construct the control point $q_i^+ := E_{p_i}(v_i) \cdot p_i$. Similarly, we use v_{i+1} to construct the point $q_{i+1}^- := E_{p_{i+1}}(-v_{i+1}) \cdot p_{i+1}$. We can then construct a cubic Bézier curve from the four points p_i, q_i^+, q_{i+1}^-, p_{i+1} as indicated in Figure 1. If the velocities v_i are chosen following Theorem 2.2, the resulting piecewise cubic curve will have optimal regularity.

where

$$\boldsymbol{w}(\boldsymbol{\xi}) := (w_1(\xi_0, \xi_1, \xi_2), \dots, w_{N-1}(\xi_{N-2}, \xi_{N-1}, \xi_N)), \tag{23}$$

and $\langle \varpi, \boldsymbol{v} \rangle$ is the componentwise application of the connection ϖ. Pseudo code for the complete algorithm is given in Algorithm 1. We consider two options for boundary conditions.

(i) Clamped spline:

$$v_0(v) = v_{\text{start}}, \qquad v_N(v) = v_{\text{end}} \tag{24}$$

where v_{start} and v_{end} are prescribed constants.

(ii) Natural spline:

$$v_0(v) = \frac{1}{2} \log_{p_0}(q_1^-), \qquad v_N(v) = -\frac{1}{2} \log_{p_N}(q_{N-1}^+). \tag{25}$$

3.1. **Convergence result.** In this section we give a result on convergence of the fixed point method given by Algorithm 1. To do so, we first give some preliminary definition.

The Riemannian distance between $p, q \in M$ is denoted $d(p, q)$. Our proof of convergence uses that any two consecutive points p_i, p_{i+1} are close enough. Thus, we define the constant

$$D = \max_{0 \le i \le N-1} d(p_i, p_{i+1}). \tag{26}$$

The other constant that comes into play is a bound on (essentially) the curvature of M. Indeed, if $\|\cdot\|_p$ denotes the H_p-invariant norm on $\mathfrak{m}_p$ associated with the Riemannian structure of M, then we define the constant $K \ge 0$ as

$$K^2 = \sup_{\xi, \eta, \zeta \in \mathfrak{m}_p \setminus 0} \frac{\|[\xi, [\eta, \zeta]]\|}{\|\xi\| \|\eta\| \|\zeta\|}. \tag{27}$$

If M is flat, then $K = 0$. If M is the n-sphere of radius r, then $K = 1/r$.

Our convergence result is now formulated as follows.

Algorithm 1 Computing the control points q_i^+ and q_i^-

The auxiliary functions E and log are defined in (15) and (16).

$\boldsymbol{v} \leftarrow (0, \dots, 0)$
repeat
  $\bar{\boldsymbol{v}} \leftarrow (v_0(v), \boldsymbol{v}, v_N(v))$ ▷ v_0 and v_N are determined by (24) or (25)
  for $i \leftarrow 0, \dots, N-1$ **do**
    $g_i^+ \leftarrow E_{p_i}(\bar{v}_i)$
    $q_i^+ \leftarrow g_i^+ \cdot p_i$
  end for
  for $i \leftarrow 1, \dots, N$ **do**
    $g_i^- \leftarrow E_{p_i}(-\bar{v}_i)$
    $q_i^- \leftarrow g_i^- \cdot p_i$
  end for
  for $i \leftarrow 1, \dots, N-1$ **do**
    $\delta_i \leftarrow \log_{p_i}(g_i^- \cdot q_{i+1}^-) - \log_{p_i}(g_i^+ \cdot q_{i-1}^+) - 2v_i$
    $v_i \leftarrow v_i + \frac{1}{4}\delta_i$
  end for
until $\|\delta\| \le TOL$

The outcome is the control points q_i^+ and q_i^-, from which one can compute the spline segments.

Theorem 3.1. *If KD is sufficiently small, then Algorithm 1 with natural boundary conditions converges linearly. If KD and $\max\{ K\|v_0\|, K\|v_N\| \}$ are both sufficiently small, then Algorithm 1 with clamped boundary conditions converges linearly.*

Outline of proof. Again, the proof is long and technical, and therefore given in Appendix C. Here we give a brief outline.

The proof is based on showing that the iteration mapping (22) is a contraction. For convenience, we use the variables $\xi_i \in \mathfrak{m}_{p_i}$ instead of $v_i \in T_{p_i}M$. The iteration mapping is denoted ϕ.

(1) The first step is to give an invariant region of the iteration mapping. This is given in Proposition C.1, which proves existence of $V > 0$ (depending on both D and K), such that $\|\boldsymbol{\xi}\| \le V$ implies $\|\phi(\boldsymbol{\xi})\| \le V$.
(2) The next step is to prove that ϕ is a contraction, which is established by a series of estimated on the partial derivatives on ϕ (Proposition C.4, Proposition C.3, and Proposition C.6). These estimates depend on K.
(3) The final step, in § C.3, consists in using the contraction mapping theorem to obtain linear convergence.

□

4. Examples

4.1. **Unit quaternions.** Unit quaternions (versors) are used extensively in computer graphics to represent 3-D rotations. They are elements of the form $q = q_0 + q_1 i + q_2 j + q_3 k$

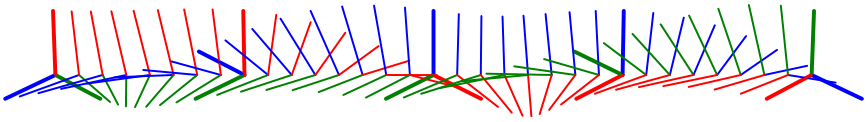

FIGURE 5. Interpolation between 5 orientations, illustrated by the orientation of the frame consisting of the axes i (red), j (green), and k (blue). The bold frames mark the interpolants.

with

$$q_0^2 + q_1^2 + q_2^2 + q_3^2 = 1. \tag{28}$$

Thus, we can identify unit quaternions with S^3. In turn, S^3 is a double cover of $\mathrm{SO}(3)$. Thus, a point on S^3 gives a rotation matrix, and likewise any rotation matrix corresponds to two antipodal points on S^3. The rotation of a vector $p = (p_x, p_y, p_z)$ by a unit quaternion q can be compactly written using quaternion multiplication as

$$\mathrm{rot}_q(p) = qpq^{-1}$$

where $p = p_x i + p_y j + p_z k$ is thought of as a pure imaginary quaternion.

Since $S^3 \simeq \mathrm{O}(4)/\mathrm{O}(3)$ is a Riemannian symmetric space (with respect to the standard Riemannian metric), we can use Algorithm 1 to obtain C^2-continuous spline interpolation between rotations. Since geodesics on S^3 are given by great circles, it is straightforward to derive the mappings E and log.

The resulting C^2-curve interpolating 5 orientations is shown in Figure 5. In the figure, an element $\gamma(t) \in S^3$ is represented by the rotated basis vectors

$$\{\, \mathrm{rot}_{\gamma(t)}(i), \mathrm{rot}_{\gamma(t)}(j), \mathrm{rot}_{\gamma(t)}(k) \,\}.$$

The actual interpolation points are marked with bolder lines.

4.2. **Quantum states.** The control of quantum states is an important subproblem in quantum information and the realization of quantum computers [3]. The objective is to find a time-dependent Hamiltonian $H(t)$ designed to 'steer' a given quantum state $|\psi_0\rangle$ through a sequence of states $|\psi_1\rangle, |\psi_2\rangle, \ldots, |\psi_N\rangle$ at given times $t_1, \ldots, t_N$. As instantaneous switching of the Hamiltonian is not experimentally feasible [1], the interpolating curve $|\psi(t)\rangle$ should be at least C^2 continuous.

If the quantum state space is finite dimensional, corresponding to an ensemble of qubits, then, in the geometric description of quantum mechanics [6, 7], the phase space is given by complex projective space $\mathbb{C}P^n$. The quantum control problem can then be seen as a two-step process:

(1) Find an interpolating curve $t \mapsto |\psi(t)\rangle \in \mathbb{C}P^n$ such that $|\psi(0)\rangle = |\psi_0\rangle$ and $|\psi(t_k)\rangle = |\psi_k\rangle$.
(2) Using the homogeneous structure $\mathbb{C}P^n \simeq \mathrm{U}(n+1)/\mathrm{U}(n) \times \mathrm{U}(1)$, lift $|\psi(t)\rangle$ to a curve $t \mapsto g(t) \in \mathrm{U}(n+1)$ such that $g(0) = e$ and $\pi(g(t)) = |\psi(t)\rangle$.[1] The time-dependent Hamiltonian is then given by $H(t) = -i\dot{g}(t)g(t)^{-1}$.

[1]The lifting is, of course, not unique. It is natural to minimize the change in Hamiltonian $\dot{H}$, as suggested by Brody, Holm, and Meier [1].

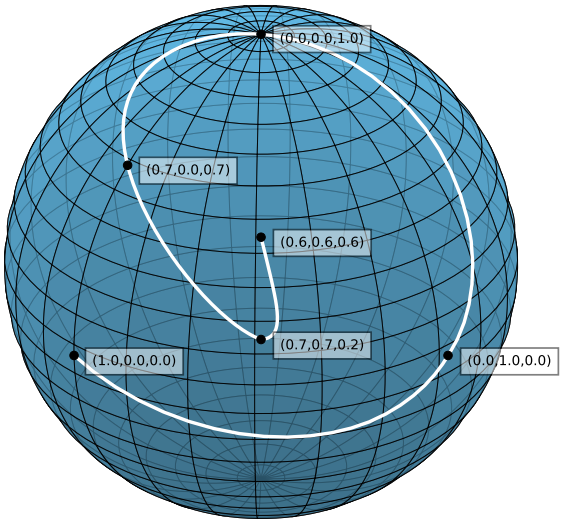

FIGURE 6. Interpolation between 6 qubit states visualized on the Bloch sphere. The resulting curve is C^2 and therefore generated by a time-dependent Hamiltonian $iH(t) \in \mathfrak{u}(n+1)$ where $t \mapsto \dot{H}(t)$ is continuous.

We can use Algorithm 1 for the first step. (The second step is not treated in this paper.)

The simplest case of a single qubit corresponds to the phase space $\mathbb{C}P^1$, which is isomorphic to a sphere (called the *Bloch sphere*). Using 6 interpolation points, the resulting interpolating curve is visualized on the Bloch sphere in Figure 6.

4.3. **Affine shapes.** In computer vision, an *affine shape* is an orbit of the joint action of the affine group on a set of points. It turns out that for $k+1$ points with full affine range in a space of dimension n, the affine shapes are in one-to-one correspondence with the points on the Grassmannian $\mathrm{Gr}(n,k)$ [5], that is, the set of subspaces of dimension n in $\mathbb{R}^k$.

In the example of Figure 7, to the affine shape of four points which span the plane $\mathbb{R}^2$ we associate a point in $\mathrm{Gr}(2,3)$.

Let us describe the mapping from an affine shape to a point on a Grassmannian. We assume for simplicity that the $k+1$ points $p_0, \dots, p_k$ affinely span the whole space of dimension n. Choose a coordinate system, and place the coordinates of the vectors $p_1 - p_0, \dots, p_k - p_0$ column by column in a $n \times k$ matrix. The kernel of this matrix is then a subspace of $\mathbb{R}^k$.

Assuming that the points span the whole space is akin to assume that the matrix has full rank, in other words, the kernel has dimension $k-n$. This gives us a point in $\mathrm{Gr}(k-n,k)$, which, by canonical isomorphism between $\mathrm{Gr}(k-n,k)$ and $\mathrm{Gr}(n,k)$, gives a point in $\mathrm{Gr}(n,k)$.

Let us study the particular case of the shapes described on Figure 7. In this case, the ambient space has dimension 2, and there are $3+1$ points. This means that, for every shape, we obtain a matrix of shape 2×3, which has full rank. For every shape, we thus obtain a kernel of dimension one, that is, a direction, in $\mathbb{R}^3$. We see that the set of shape is isomorphic to the real projective plane $\mathbb{R}P^2$.

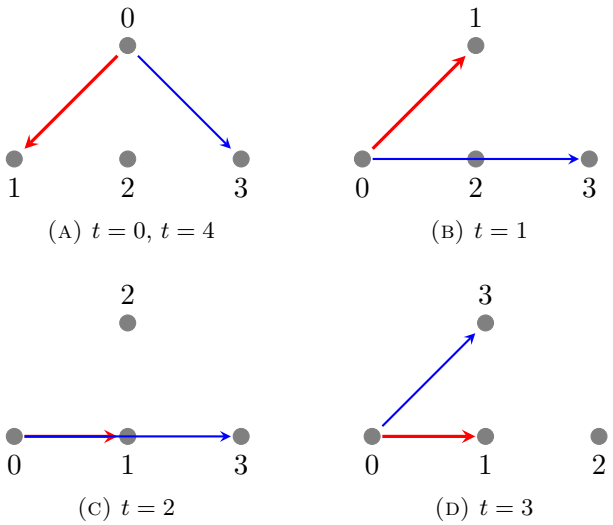

FIGURE 7. Four affine shapes that we interpolate. During the reconstruction, we form a basis with the points 0, 1 and 3 (the thicker axis is the first basis vector, while the thinner one is the second basis vector). At time 2, the basis is degenerate, so in that coordinate system, we expect the point 2 to go to infinity.

We visualise the corresponding points as follows. First, we compute the intersection of the kernel direction with the half-sphere

$$\{\, (x, y, z) \in \mathbb{R}^2 \mid z \leq 0 \,\}. \tag{29}$$

We then compute the stereographic projection from the point of coordinate $(0, 0, 1)$. This function is explicitly given by

$$(x, y, z) \mapsto \Big(\frac{x}{1-z}, \frac{y}{1-z}\Big). \tag{30}$$

We now interpolate the shapes on Figure 7, considered as points on $\mathbb{R}P^2$. We plot the resulting curve on Figure 10.

5. Outlook

There are a number of possible extensions of our methods and proofs to be studied in future work. Here we list some of them.

- We surmise that the conditions of Theorem 2.2 are in fact valid for more general symmetric spaces than Riemannian ones. In particular, we would like to be able to prove that result directly, without resorting to the previous result of Popiel and Noakes, which is the only reason for us to restrict to the *Riemannian* symmetric space case at this point.
- The only structure that we need to implement Algorithm 1 and to state Theorem 2.2 is an invariant connection (see (6a)), which only requires the homogeneous space at hand to be *reductive* [10, § 4]. We would expect similar results in that

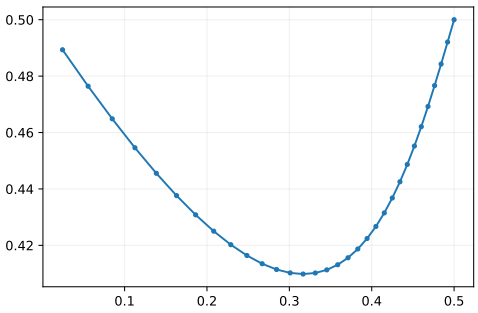

FIGURE 8. A plot of the point labeled 2 in Figure 7 between time 0 and 1. At time 0, the point is at coordinate $(0.5, 0.5)$, at time 1, the coordinate is $(0, 0.5)$.

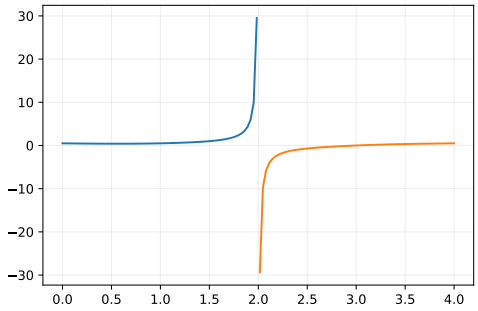

FIGURE 9. We plot the y coordinate of point 2 in Figure 7. As expected, at time 2, the coordinate is infinite. Note how the coordinate changes sign. This effect is only apparent during reconstruction, as nothing is infinite in the actual computed spline curve, as shown on Figure 10.

case, which would for instance cover arbitrary Lie groups, as well as Stiefel manifolds.

- A modification of our algorithm is possible in the more general case of *arbitrary* Riemannian manifolds (not necessarily symmetric), using the original C^2 condition of Popiel and Noakes [14]. We are working on an implementation and a proof of convergence.
- Our algorithm is currently based on a fixed point iteration. One could instead use a Newton iteration, which would ensure convergence in one step in the Euclidean case.

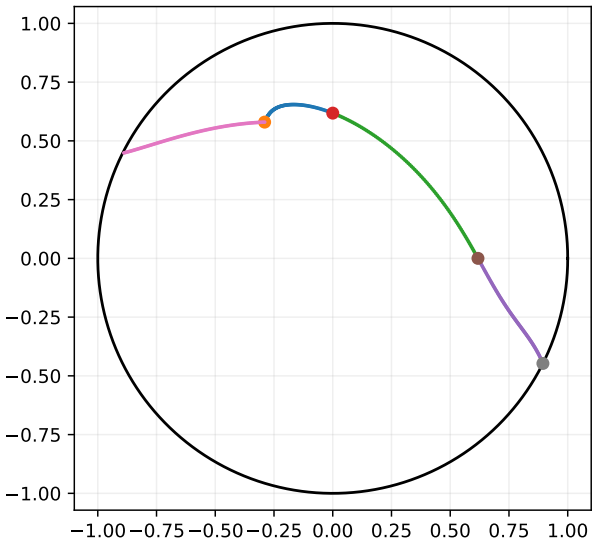

.

FIGURE 10. A stereographic projection of the spline obtained from interpolating the shapes of Figure 7. As we identify any two opposite points of the circle, the curve is closed. It is also apparent, that there are no coordinate systems in which the curve would appear on only one half of the sphere. This means that any choice of basis would give a plot similar to Figure 9, with some coordinate going to infinity.

ACKNOWLEDGMENTS

This project has received funding from the European Union's Horizon 2020 research and innovation programme under grant agreement No 661482, from the Swedish Foundation for Strategic Research under grant agreement ICA12-0052, and from the Knut and Alice Wallenberg Foundation under grant agreement KAW-2014.0354.

APPENDIX A. IDENTITIES AND BOUNDS ON SYMMETRIC SPACES

We prove several identities and bounds valid on (Riemannian) symmetric spaces.

Let $M = G/H_p$ be a symmetric space, where $p \in M$ and $\mathfrak{g} = \mathfrak{m}_p \oplus \mathfrak{h}_p$ is the decomposition of § 2.1, and let $\pi_p : \mathfrak{g} \to \mathfrak{m}_p$ be the canonical projection. Recall that the connection ϖ is defined so that, for all $p \in M, \xi \in \mathfrak{g}$,

$$\langle \varpi, \xi \cdot p \rangle = \pi_p(\xi) \in \mathfrak{m}_p \tag{31}$$

Throughout this section and the following, dexp denotes the trivialized derivative of the Lie group exponential, that is

$$\mathbf{T} \exp_\xi(\delta\xi) = \operatorname{dexp}_\xi(\delta\xi) \cdot \exp(\xi) = \exp(\xi) \cdot \operatorname{dexp}_{-\xi}(\delta\xi)$$

(where the last equality follows from differentiating $\exp(\xi)\exp(-\xi) = \mathrm{id}$.)

Lemma A.1. *Let $\xi, \delta\xi \in \mathfrak{g}$, then*

$$\frac{\partial}{\partial \xi}(\exp(\xi)\cdot p)\delta\xi = \exp(\xi)\cdot(\pi_p \circ \operatorname{dexp}_{-\xi})(\delta\xi)\cdot p.$$

Proof. By differentiating $\exp(\xi)\cdot p$ we get

$$\begin{aligned}\frac{\partial}{\partial \xi}(\exp(\xi)\cdot p)\delta\xi &= \exp(\xi)\cdot \operatorname{dexp}_{-\xi}(\delta\xi)\cdot p \\ &= \exp(\xi)\cdot(\pi_p \circ \operatorname{dexp}_{-\xi})(\delta\xi)\cdot p\end{aligned}$$

where the second equality is because $\pi_p(\eta)\cdot p = \eta \cdot p$ for all $\eta \in \mathfrak{g}$. □

Lemma A.2. *Let $\xi, \eta \in \mathfrak{m}_p$, then*

$$\pi_p \circ \operatorname{dexp}_{-\xi}(\eta) = \frac{\sinh(\operatorname{ad}_\xi)}{\operatorname{ad}_\xi}(\eta) = \pi_p \circ \operatorname{dexp}_{\xi}(\eta).$$

Proof. As a function $\mathfrak{g} \to \mathfrak{g}$, dexp_ξ is an analytic function of ad_ξ with Taylor series $\operatorname{dexp}_\xi = \sum_{k=0}^{\infty} \frac{1}{(k+1)!}\operatorname{ad}_\xi^k$. When applied to an element in $\eta \in \mathfrak{m}_p$, we have that

$$\operatorname{ad}_\xi^k \eta \in \begin{cases} \mathfrak{m}_p & k \text{ even} \\ \mathfrak{h}_p & k \text{ odd} \end{cases}$$

The effect of π_p is to eliminate terms in $\mathfrak{h}_p$, leaving only the even part

$$\pi_p \circ \operatorname{dexp}_\xi \eta = \sum_{l=0}^{\infty} \frac{1}{(2l+1)!}\operatorname{ad}_\xi^{2l}\eta = \frac{\sinh(\operatorname{ad}_\xi)}{\operatorname{ad}_\xi}\eta,$$

which does not depend on the sign of ξ.

□

Lemma A.3. *Let I be the involution at p, i.e., $I(q) = E_p(-\log_p(q))$, and let $\xi \in \mathfrak{m}_p$, $w \in \mathbf{T}_pM$. Then*

$$\mathbf{T}I_{\exp(\xi)\cdot p}(\exp(\xi)\cdot w) = -\exp(-\xi)\cdot w.$$

Proof. Let $q(\xi) = \exp(\xi)\cdot p$ for $\xi \in \mathfrak{m}_p$. Then $q : \mathfrak{m}_p \to M$ is a local diffeomorphism and $I(q(\xi)) = \exp(-\xi)\cdot p$. Differentiating both $q(\xi)$ and $I(q(\xi))$ with respect to ξ, and using Lemma A.1, we get

$$\begin{aligned}\mathbf{T}q_\xi(\eta) &= \exp(\xi)\cdot(\pi \circ \operatorname{dexp}_{-\xi}(\eta))\cdot p \\ \mathbf{T}I_{q(\xi)} \circ \mathbf{T}q_\xi(\eta) &= -\exp(-\xi)\cdot(\pi \circ \operatorname{dexp}_{\xi}(\eta))\cdot p.\end{aligned}$$

Since q is a diffeomorphism, we can choose η such that $\mathbf{T}q_\xi(\eta) = \exp(\xi)\cdot w$, *i.e.*, $w = \pi \circ \operatorname{dexp}_{-\xi}(\eta)\cdot p$. Using Lemma A.2, we also have $w = \pi \circ \operatorname{dexp}_{\xi}(\eta)\cdot p$, and the result follows. □

Lemma A.4. *Let $g \in G$, and $q \in M$. Then*

$$\log_{g\cdot p}(q) = g\cdot \log_p(g^{-1}\cdot q).$$

Proof. Let $\omega = \langle \varpi, \log_p(g^{-1} \cdot q) \rangle_p$. Then $g \exp(\omega) \cdot p = q$. On the other hand, we have

$$g \cdot \omega \cdot p = \mathrm{Ad}_g(\omega) \cdot g \cdot p,$$

where $\mathrm{Ad}_g(\omega) \in \mathfrak{m}_{g \cdot p}$, and

$$\exp(\mathrm{Ad}_g(\omega)) \cdot g \cdot p = g \exp(\omega) \cdot p = q.$$

We therefore conclude that

$$\begin{aligned} \log_{g \cdot p}(q) &= \mathrm{Ad}_g(\omega) \cdot g \cdot p \\ &= g \cdot \omega \cdot p \\ &= g \cdot \log_p(g^{-1} \cdot q). \end{aligned}$$

□

For the final lemmata, we assume $M = G/H_p$ to be a Riemannian symmetric space. This is equivalent to the existence of an H_p-invariant inner product on $\mathfrak{m}_p$, from which we derive a norm $\|\cdot\|$ on $\mathfrak{m}_p$.

Lemma A.5. *Let $\xi, \eta \in \mathfrak{m}_p$, then*

$$\begin{aligned} \|\pi_p \circ \mathrm{dexp}_\xi(\eta)\| &= \left\| \frac{\sinh(\mathrm{ad}_\xi)}{\mathrm{ad}_\xi}(\eta) \right\| \leq \frac{\sinh(K\|\xi\|)}{K\|\xi\|} \|\eta\|, \\ \|(\pi_p \circ \mathrm{dexp}_\xi)^{-1}(\eta)\| &= \left\| \frac{\mathrm{ad}_\xi}{\sinh(\mathrm{ad}_\xi)}(\eta) \right\| \leq \frac{K\|\xi\|}{\sin(K\|\xi\|)} \|\eta\|. \end{aligned}$$

(Notice sin*, not* sinh *in the last denominator)*

Proof. We use Lemma A.2 to set $\pi \circ \mathrm{dexp}_\xi = \frac{\sinh(\mathrm{ad}_\xi)}{\mathrm{ad}_\xi}$ The lemma follows from considering the infinite series for $\frac{\sinh(\mathrm{ad}_\xi)}{\mathrm{ad}_\xi}$ and its inverse, as well as the definition of K. □

Lemma A.6. *Let $\xi_0, \xi_1 \in \mathfrak{m}_p$, $q_0 = E_p(\xi_0) \cdot p$ and $q_1 = E_p(\xi_1) \cdot p$. Then the inequality*

$$\|\xi_0 - \xi_1\| \leq \frac{KU}{\sin(KU)} d(q_0, q_1),$$

where $U = \frac{1}{2}(\|\xi_0\| + \|\xi_1\| + d(q_0, q_1))$, holds.

Proof. Let $\gamma(t)$ be the geodesic from $\gamma(0) = q_0$ to $\gamma(1) = q_1$, and let $\alpha(t) \in \mathfrak{m}_p$ be such that

$$\exp(\alpha(t)) \cdot p = \gamma(t). \tag{32}$$

Then $\xi_0 = \alpha(0)$, $\xi_1 = \alpha(1)$. We note that, by the triangle inequality, we have

$$\begin{aligned} \|\alpha(t)\| = d(p, \gamma(t)) &\leq \min\{\|\xi_0\| + t d(q_0, q_1), \|\xi_1\| + (1-t) d(q_0, q_1)\} \\ &\leq \frac{1}{2}(\|\xi_0\| + \|\xi_1\| + d(q_0, q_1)) = U \end{aligned} . \tag{33}$$

Differentiating (32) we get

$$\exp(\alpha(t)) \cdot (\mathrm{dexp}_{-\alpha(t)} \dot{\alpha}(t)) \cdot p = \dot{\gamma}(t)$$

or

$$(\pi_p \circ \mathrm{dexp}_{-\alpha(t)}) \dot{\alpha}(t) \cdot p = \exp(-\alpha(t)) \cdot \dot{\gamma}(t),$$

where we have used that $\pi_p(\eta)\cdot p = \eta\cdot p$ for all $\eta\in\mathfrak{g}$. Taking norms on both sides, using that G acts by isometries, we have

$$\|(\pi_p\circ \operatorname{dexp}_{-\alpha(t)})\dot\alpha(t)\| = \|\dot\gamma(t)\| = d(q_0,q_1),$$

and, by Lemma A.5

$$\|\dot\alpha(t)\| \le \frac{K\|\alpha(t)\|}{\sin(K\|\alpha(t)\|)} d(q_0,q_1)$$

We now use the monotonicity of $x/\sin x$, and the bound Equation 33 to obtain

$$\begin{aligned}\|\alpha(1)-\alpha(0)\| &\le \int_0^1 \|\dot\alpha(t)\|\mathrm{d}t\\ &\le \int_0^1 \frac{K\|\alpha(t)\|}{\sin(K\|\alpha(t)\|)}\mathrm{d}t d(q_0,q_1)\\ &\le \frac{KU}{\sin(KU)} d(q_0,q_1)\end{aligned}$$

□

Appendix B. C^2 continuity

We now prove Theorem 2.2. The proof relies on a result by Popiel and Noakes [14].

Proof of Theorem 2.2. At non-integer t, the spline is always C^∞. We show that the spline is C^2 at $t=i\in\{1,2,\dots,N-1\}$ (i.e. when the spline is interpolating p_i). By [14, Thm. 3], a sufficient and necessary condition for the spline to be C^2 at $t=i$ is

$$\mathbf{T}I_{q_i^+}(\log_{q_i^+} q_{i+1}^-) = -\log_{q_i^-}(q_{i-1}^+) - 2\log_{q_i^-}(p_i) \tag{34}$$

We proceed by removing the dependence of $\mathbf{T}I$ in (34) by using the lemmata from Appendix A.

By Lemma A.4, we have

$$\begin{aligned}\log_{q_i^+}(q_{i+1}^-) &= \log_{\exp(\xi_i)\cdot p_i}(q_{i+1}^-)\\ &= \exp(\xi_i)\cdot\log_{p_i}(\exp(-\xi_i)\cdot q_{i+1}^-),\\ \log_{q_i^-}(q_{i-1}^+) &= \log_{\exp(-\xi_i)\cdot p_i}(q_{i-1}^+)\\ &= \exp(-\xi_i)\cdot\log_{p_i}(\exp(\xi_i)\cdot q_{i-1}^+).\end{aligned}$$

Using Lemma A.3, with $w=\log_{p_i}(\exp(-\xi_i)\cdot q_{i+1}^-)$, we can write

$$\begin{aligned}\mathbf{T}I_{q_i^+}(\log_{q_i^+} q_{i+1}^-) &= \mathbf{T}I_{\exp\xi_i\cdot p_i}(\exp(\xi_i)\cdot\log_{p_i}(\exp(-\xi_i)\cdot q_{i+1}^-)\\ &= -\exp(-\xi_i)\cdot\log_{p_i}(\exp(-\xi_i)\cdot q_{i+1}^-).\end{aligned} \tag{35}$$

Next, we note that

$$\log_{q_i^-}(p_i) = \exp(-\xi_i)\cdot v_i. \tag{36}$$

Using (35) and (36), we can rewrite (34) as

$$-\exp(-\xi_i)\cdot\log_{p_i}(\exp(-\xi_i)\cdot q_{i+1}^-) = -\exp(-\xi_i)\cdot\log_{p_i}(\exp(\xi_i)\cdot\exp(\xi_{i-1})\cdot p_{i-1}) - 2\exp(-\xi_i)\cdot v_i.$$

Acting on the whole equation from the left with $\exp(\xi_i)$ and rearranging, we get

$$\log_{p_i}(\exp(-\xi_i)\cdot q_{i+1}^-) - v_i = \log_{p_i}(\exp(\xi_i)\cdot q_{i-1}^+) + v_i.$$

Equation (18) is recovered by using (17) to replace $v_i = \log_{p_i}(q_i^+) = -\log_{p_i}(q_i^-)$.

□

Appendix C. Convergence of the fixed-point method

We now proceed to show that, if the interpolation points are sufficiently close, Algorithm 1 converges to a solution.

In the proof, we will work with variables in the Lie algebra $\mathfrak{g}$ Let $\mathfrak{m}_{\boldsymbol{p}} = \mathfrak{m}_{p_0} \times \cdots \times \mathfrak{m}_{p_N}$, and $\boldsymbol{\xi} = (\xi_0, \ldots, \xi_N) \in \mathfrak{m}_{\boldsymbol{p}}$, be the Lie algebra elements defined by $\xi_i = \langle \varpi, v_i \rangle_{p_i}$.

Switching to variables in the Lie algebra, the fixed-point iteration (22) becomes a map

$$\begin{aligned} \boldsymbol{\phi} &\colon \mathfrak{m}_{\mathbf{p}} \to \mathfrak{m}_{\mathbf{p}}, \\ \boldsymbol{\phi}(\boldsymbol{\xi}) &= (\xi_0, \ldots, \xi_N) \to (\phi_0(\boldsymbol{\xi}), \ldots, \phi_N(\boldsymbol{\xi})). \end{aligned}$$

For $1 \le i \le N-1$, $\phi_i(\boldsymbol{\xi}) = \frac{1}{4}\langle \varpi, w_i(\boldsymbol{\xi}) \rangle_{p_i} + \frac{1}{2}\xi_i$. To simplify notation, let $L_p : M \to \mathfrak{m}_p$ be defined by $L_p(q) = \langle \varpi, \log_p q \rangle_p$.

$$\phi_i(\boldsymbol{\xi}) = \frac{1}{4}(L_{p_i}(\exp(-\xi_i)\exp(-\xi_{i+1})\cdot p_{i+1}) - L_{p_i}(\exp(+\xi_i)\exp(+\xi_{i-1})\cdot p_{i-1})) + \frac{1}{2}\xi_i,$$

ϕ_0 and ϕ_N are given by the boundary conditions.

$$\phi_0(\boldsymbol{\xi}) = \langle \varpi, v_0(\boldsymbol{\xi}) \rangle, \qquad \phi_N(\boldsymbol{\xi}) = \langle \varpi, v_N(\boldsymbol{\xi}) \rangle$$

It is convenient to introduce the auxiliary variables

$$\begin{aligned} \omega_i^+(\boldsymbol{\xi}) &= \langle \varpi, w_i^+ \rangle_{p_i} = L_{p_i}\left(\exp(-\xi_i)\exp(-\xi_{i+1})\cdot p_{i+1}\right), \\ \omega_i^-(\boldsymbol{\xi}) &= \langle \varpi, w_i^- \rangle_{p_i} = L_{p_i}\left(\exp(+\xi_i)\exp(+\xi_{i-1})\cdot p_{i-1}\right), \end{aligned} \tag{37}$$

and to do a splitting $\phi_i(\boldsymbol{\xi}) = \phi_i^+(\boldsymbol{\xi}) + \phi_i^-(\boldsymbol{\xi})$, where

$$\begin{aligned} \phi_i^+(\boldsymbol{\xi}) &= \frac{1}{4}\omega_i^+(\boldsymbol{\xi}) + \frac{1}{4}v_i, \\ \phi_i^-(\boldsymbol{\xi}) &= -\frac{1}{4}\omega_i^-(\boldsymbol{\xi}) + \frac{1}{4}v_i, \end{aligned}$$

In the proof, we will require the maximum distance

$$D = \max_{0 \le i \le N-1} d(p_i, p_{i+1}),$$

and the norms

$$\|\boldsymbol{\xi}\| = \max_{0 \le i \le N} \|\xi_i\| = \max_{0 \le i \le N} \|v_i\| \tag{38}$$

and

$$\|\boldsymbol{\omega}(\boldsymbol{\xi})\| = \max_{1 \le i \le N-1} \max(\|\omega_i^+(\boldsymbol{\xi})\|, \|\omega_i^-(\boldsymbol{\xi})\|).$$

Notice that by the triangle inequality, we have

$$\|\omega_i^+(\boldsymbol{\xi})\| = d(q_i^+, q_{i+1}^-) \le d(p_i, p_{i+1}) + \|\xi_i\| + \|\xi_{i+1}\| \le D + 2\|\boldsymbol{\xi}\|$$

and similar for $\|\omega_i^-(\boldsymbol{\xi})\|$, so

$$\|\boldsymbol{\omega}(\boldsymbol{\xi})\| \le D + 2\|\boldsymbol{\xi}\| \tag{39}$$

We are now equipped to prove the convergence of the algorithm, that is Theorem 3.1 The proof consists of proving the existence of an invariant region, and thereafter bounding partial derivatives to prove that ϕ is a contraction.

C.1. **Invariant region.** We begin by establishing an invariant region.

Proposition C.1. *Let $V > 0$ satisfy the inequality*

$$\frac{1}{2}\frac{KU}{\sin(KU)}(D+V) \leq V, \tag{40}$$

where $U = D + 2V$. If

(i) *clamped spline boundary conditions are used, $\|\xi_{start}\| \leq V$, $\|\xi_{end}\| \leq V$ and $\|\boldsymbol{\xi}\| \leq V$, or,*
(ii) *natural spline boundary conditions are used and $\|\boldsymbol{\xi}\| \leq V$*

then also $\|\phi(\boldsymbol{\xi})\| \leq V$.

We first prove bounds for $\phi_i^+(\boldsymbol{\xi})$

Lemma C.2.

$$\|\phi_i^+(\boldsymbol{\xi})\| \leq \frac{1}{4}\frac{KU_i}{\sin(KU_i)}(d(p_i, p_{i+1}) + \|\xi_{i+1}\|),$$
$$\|\phi_i^-(\boldsymbol{\xi})\| \leq \frac{1}{4}\frac{KU_{i-1}}{\sin(KU_{i-1})}(d(p_i, p_{i-1}) + \|\xi_{i-1}\|),$$

where $U_i = d(p_i, p_{i+1}) + \|\xi_{i+1}\| + \|\xi_i\|$.

Proof. We prove the first inequality. The proof of the second is entirely symmetrical and is omitted.

$$\phi_i^+(\boldsymbol{\xi}) = \frac{1}{4}(\omega_i^+(\boldsymbol{\xi}) + \xi_i)$$

The proof uses Lemma A.6 to bound $\omega_i^+(\boldsymbol{\xi}) + \xi_i = \omega_i^+(\boldsymbol{\xi}) - (-\xi_i)$. A trick will simplify bounding the expressions occurring after applying the Lemma.

We have

$$\begin{aligned}\|\omega_i^+(\boldsymbol{\xi}) + \xi_i\| &= \|\mathrm{Ad}_{\exp(\xi_i)}(\omega_i^+(\boldsymbol{\xi}) + \xi_i)\| \\ &= \|\mathrm{Ad}_{\exp(\xi_i)}\omega_i^+(\boldsymbol{\xi}) + \xi_i\|.\end{aligned}$$

where $\mathrm{Ad}_{\exp(\xi_i)}\omega_i^+(\boldsymbol{\xi})$ and ξ_i are vectors in $\mathfrak{m}_{q_i^+}$.

We also have

$$\exp(-\xi_i)\cdot q_i^+ = p_i$$

and

$$\begin{aligned}\exp(\mathrm{Ad}_{\exp(\xi_i)}\omega_i^+(\boldsymbol{\xi}))\cdot q_i^+ &= \exp(\xi_i)\exp(\omega_i^+(\boldsymbol{\xi}))\exp(-\xi_i)\cdot q_i^+ \\ &= \exp(\xi_i)\exp(\omega_i^+(\boldsymbol{\xi}))\cdot p_i \\ &= \exp(-\xi_{i+1})\cdot p_{i+1} \\ &= q_{i+1}^+\end{aligned}$$

By Lemma A.6, we have

$$\|\mathrm{Ad}_{\exp(\xi_i)}\omega_i^+(\boldsymbol{\xi}) - (-\xi_i)\| \leq \frac{KT}{\sin(KT)}d(p_i, q_{i+1}^-)$$

where

$$\begin{aligned} T &= \frac{1}{2}\left(\|\mathrm{Ad}_{\exp(\xi_i)}\,\omega_i\| + \|\xi_i\| + d(p_i, q_{i+1}^-)\right) \\ &= \frac{1}{2}\left(d(q_i^+, q_{i+1}^-) + \|\xi_i\| + d(p_i, q_{i+1}^-)\right). \end{aligned}$$

From the triangle inequality, we have

$$\begin{aligned} d(q_i^+, q_{i+1}^-) &\le d(p_i, p_{i+1}) + \|\xi_i\| + \|\xi_{i+1}\| \\ d(p_i, q_{i+1}^-) &\le d(p_i, p_{i+1}) + \|\xi_{i+1}\| \end{aligned},$$

Thus $T \le U_i$, and the claim follows by the monotonicity of $\frac{x}{\sin x}$. □

Proof of Proposition C.1. Using Lemma C.2, and the inequalities $\|\xi_i\| \le \|\boldsymbol{\xi}\| \le V$, $d(p_i, p_{i+1}) \le D$ and $U_i \le U$, we get that

$$\|\phi_i(\boldsymbol{\xi})\| \le \|\phi_i^-(\boldsymbol{\xi})\| + \|\phi_i^-(\boldsymbol{\xi})\| \le \frac{1}{2}\frac{KU}{\sin(KU)}(D+V)$$

for all $1 \le i \le N-1$.

For the boundary velocities, we have,

(i) Clamped spline: $\phi_0(\boldsymbol{\xi}) = \xi_{\text{start}}$, so $\|\phi_0(\xi)\| \le V$ by our assumption.
(ii) Natural spline: $\phi_0(\boldsymbol{\xi}) = \frac{1}{2}\langle \varpi, \log_{p_0} \exp(-\xi_1)\cdot p_1\rangle_{p_0}$, so

$$\|\phi_0(\boldsymbol{\xi})\| \le \frac{1}{2}(d(p_0,p_1) + \|\xi_1\|) \le \frac{1}{2}(D+V) \le V$$

under a weaker condition on V. Similar for $\phi_N(\boldsymbol{\xi})$.

In conclusion, under the assumption (40), we have

$$\|\phi(\boldsymbol{\xi})\| = \max_{0\le i\le N} \|\phi_i(\boldsymbol{\xi})\| \le V$$

and $\left\{\, \boldsymbol{\xi} \;\middle|\; \|\boldsymbol{\xi}\| \le V \,\right\}$ forms an invariant region. □

C.2. **Contraction.** We now establish that, for D and $\|\boldsymbol{\xi}\|$ sufficiently small, $\|\mathbf{T}\phi\| \le \alpha < 1$ in the operator norm derived from Equation 38. We first consider the effect of varying ξ_{i+1} and ξ_{i-1} in $\phi_i(\boldsymbol{\xi})$.

Proposition C.3.

$$\begin{aligned} \left\|\frac{\partial \phi_i(\boldsymbol{\xi})}{\partial \xi_{i+1}}\right\| &\le \frac{1}{4}\left\|(\pi_{p_i}\circ \mathrm{dexp}_{-\omega_i^+(\boldsymbol{\xi})})^{-1}\right\|\left\|(\pi_{p_{i+1}}\circ \mathrm{dexp}_{\xi_{i+1}})\right\| \\ &\le \frac{1}{4}\frac{K\|\omega_i^+(\boldsymbol{\xi})\|}{\sin(K\|\omega_i^+(\boldsymbol{\xi})\|)}\frac{\sinh(K\|\xi_{i+1}\|)}{K\|\xi_{i+1}\|}, \end{aligned}$$

and

$$\begin{aligned} \left\|\frac{\partial \phi_i(\boldsymbol{\xi})}{\partial \xi_{i-1}}\right\| &\le \frac{1}{4}\|(\pi_{p_i}\circ \mathrm{dexp}_{-\omega_i^-(\boldsymbol{\xi})})^{-1}\|\|(\pi_{p_{i-1}}\circ \mathrm{dexp}_{\xi_{i-1}})\| \\ &\le \frac{1}{4}\frac{K\|\omega_i^-(\boldsymbol{\xi})\|}{\sin(K\|\omega_i^-(\boldsymbol{\xi})\|)}\frac{\sinh(K\|\xi_{i-1}\|)}{K\|\xi_{i-1}\|}, \end{aligned}$$

Proof. We only prove the first claim. The proof of the second is entirely symmetrical. ξ_{i+1} only enters $\phi_i(\boldsymbol{\xi})$ through the term $\frac{1}{4}\omega_i^+(\boldsymbol{\xi})$, thus $\frac{\partial \phi_i(\boldsymbol{\xi})}{\partial \xi_{i+1}} = \frac{1}{4}\frac{\partial \omega_i^+(\boldsymbol{\xi})}{\partial \xi_{i+1}}$

By the definition of $\omega_i^+(\boldsymbol{\xi})$, we have

$$\exp(\omega_i^+(\boldsymbol{\xi})) \cdot p_i = \exp(-\xi_i)\exp(-\xi_{i+1}) \cdot p_{i+1}$$

Differentiating implicitly on both sides, then acting from the left by $\exp(-\omega_i^+(\boldsymbol{\xi}))$, we get

$$(\operatorname{dexp}_{-\omega_i^+(\boldsymbol{\xi})} \delta\omega_i^+) \cdot p_i = -\exp(-\omega_i^+(\boldsymbol{\xi}))\exp(-\xi_i)\exp(-\xi_{i+1}) \cdot (\operatorname{dexp}_{\xi_{i+1}} \delta\xi_{i+1}) \cdot p_{i+1}$$

Since G acts by isometries, we have that

$$\|(\operatorname{dexp}_{-\omega_i^+(\boldsymbol{\xi})} \delta\omega_i^+) \cdot p_i\| = \|(\operatorname{dexp}_{\xi_{i+1}} \delta\xi_{i+1}) \cdot p_{i+1}\|.$$

$$\|\pi_{p_i} \circ \operatorname{dexp}_{-\omega_i^+(\boldsymbol{\xi})}(\delta\omega_i^+)\| = \|\pi_{p_{i+1}} \circ \operatorname{dexp}_{\xi_{i+1}}(\delta\xi_{i+1})\|.$$

It follows that

$$\|\delta\omega_i^+\| \leq \|(\pi_{p_i} \circ \operatorname{dexp}_{-\omega_i^+(\boldsymbol{\xi})})^{-1}\| \|\pi_{p_{i+1}} \circ \operatorname{dexp}_{\xi_{i+1}}\| \|\delta\xi_{i+1}\|.$$

The last inequality in the claim follows from Lemma A.5. □

We note that we can also use a Taylor expansion of the right hand side to get the asymptotic bound

$$\left\| \frac{\partial \phi_i(\boldsymbol{\xi})}{\partial \xi_{i+1}} \right\| \leq 1 + \frac{1}{6}K^2\|\omega_i^+(\boldsymbol{\xi})\|^2 + \frac{1}{6}K^2\|\xi_i\|^2 + \mathcal{O}(K^4\|\omega_i^+(\boldsymbol{\xi})\|^4, K^4\|\boldsymbol{\xi}\|^4),$$

To bound $\frac{\partial \phi_i(\boldsymbol{\xi})}{\partial \xi_i}$, it is again advantageous to do the splitting $\phi_i(\boldsymbol{\xi}) = \phi_i^+(\boldsymbol{\xi}) + \phi_i^-(\boldsymbol{\xi})$, and consider each term separately.

While it is possible to bound $\left\| \frac{\partial \phi_i^+(\boldsymbol{\xi})}{\partial \xi_i} \right\|$ by trigonometric and hyperbolic functions of $K\|\xi_i\|$ and $K\|\omega_i^+(\boldsymbol{\xi})\|$, the required calculations are lengthy, and we restrict ourself to an asymptotic bound.

Proposition C.4.

$$\left\| \frac{\partial \phi_i^+(\boldsymbol{\xi})}{\partial \xi_i} \right\| \leq \frac{1}{4}K^2 \left(\frac{1}{3}\|\omega_i^+(\boldsymbol{\xi})\|^2 + \frac{1}{6}\|\xi_i\|^2 + \frac{1}{2}\|\xi_i\|\|\omega_i^+(\boldsymbol{\xi})\| \right) + \mathcal{O}(K^4\|\omega_i^+(\boldsymbol{\xi})\|^4, K^4\|\xi_i\|^4)$$

and

$$\left\| \frac{\partial \phi_i^-(\boldsymbol{\xi})}{\partial \xi_i} \right\| \leq \frac{1}{4}K^2 \left(\frac{1}{3}\|\omega_i^-(\boldsymbol{\xi})\|^2 + \frac{1}{6}\|\xi_i\|^2 + \frac{1}{2}\|\xi_i\|\|\omega_i^-(\boldsymbol{\xi})\| \right) + \mathcal{O}(K^4\|\omega_i^-(\boldsymbol{\xi})\|^4, K^4\|\xi_i\|^4)$$

Again, we will only prove the first claim, the proof of the second is entirely symmetrical. We first prove a lemma.

Lemma C.5.

$$\frac{\partial \omega_i^+(\boldsymbol{\xi})}{\partial \xi_i}(\delta\xi_i) = -(\pi_{p_i} \circ \operatorname{dexp}_{-\omega_i^+(\boldsymbol{\xi})})^{-1} \circ (\pi_{p_i} \circ \operatorname{Ad}_{\exp(-\omega_i^+(\boldsymbol{\xi}))} \circ \operatorname{dexp}_{-\xi_i})\delta\xi_i.$$

Proof. We use that

$$\exp(\omega_i^+(\boldsymbol{\xi}))\cdot p_i = \exp(-\xi_i)\cdot q_{i+1}^- \tag{41}$$

By differentiating implicitly, we get

$$\begin{aligned}\exp(\omega_i^+(\boldsymbol{\xi}))\cdot(\operatorname{dexp}_{-\omega_i^+(\boldsymbol{\xi})}\delta\omega_i^+)\cdot p_i &= -(\operatorname{dexp}_{-\xi_i}\delta\xi_i)\cdot\exp(-\xi_i)\cdot q_{i+1}^- \\ &= -(\operatorname{dexp}_{-\xi_i}\delta\xi_i)\cdot\exp(\omega_i^+(\boldsymbol{\xi}))\cdot p_i,\end{aligned}$$

where the second equality uses (41). Acting from the left with $\exp(-\omega_i^+(\boldsymbol{\xi}))$, we get

$$(\operatorname{dexp}_{-\omega_i^+(\boldsymbol{\xi})}\delta\omega_i^+(\boldsymbol{\xi}))\cdot p_i = -\operatorname{Ad}_{\exp(-\omega_i^+(\boldsymbol{\xi}))}\circ\operatorname{dexp}_{-\xi_i}(\delta\xi)\cdot p_i$$

Applying the connection ϖ to both sides, we get

$$\left(\pi_{p_i}\circ\operatorname{dexp}_{-\omega_i^+(\boldsymbol{\xi})}\right)\delta\omega_i^+ = -\left(\pi_{p_i}\circ\operatorname{Ad}_{\exp(-\omega_i^+(\boldsymbol{\xi}))}\circ\operatorname{dexp}_{-\xi_i}\right)\delta\xi_i,$$

where the bracketed expressions are linear operators $\mathfrak{m}_{p_i}\to\mathfrak{m}_{p_i}$. $\left(\pi_{p_i}\circ\operatorname{dexp}_{-\omega_i^+(\boldsymbol{\xi})}\right)$ is invertible by Lemma A.2 , and the claim follows. □

We now proceed with the proof of the proposition

Proof. From the definition of ϕ_i^+,

$$\frac{\partial\phi_i^+(\boldsymbol{\xi})}{\partial\xi_i}(\delta\xi_i) = \frac{1}{4}\left(\delta\xi_i + \frac{\partial\omega_i^+(\boldsymbol{\xi})}{\partial\xi_i}(\delta\xi_i)\right)$$

Using the lemma, we have

$$\frac{\partial\phi_i^+(\boldsymbol{\xi})}{\partial\xi_i}\delta\xi_i = \frac{1}{4}\left(\delta\xi_i - (\pi_{p_i}\circ\operatorname{dexp}_{-\omega_i^+(\boldsymbol{\xi})})^{-1}\circ(\pi_{p_i}\circ\operatorname{Ad}_{\exp(-\omega_i^+(\boldsymbol{\xi}))}\circ\operatorname{dexp}_{-\xi_i})(\delta\xi_i)\right) \tag{42}$$

Using Lemma A.2, and the series expansions for $\operatorname{Ad}_{\exp(-\omega_i^+(\boldsymbol{\xi}))} = \exp(-\operatorname{ad}_{\omega_i^+})$ and $\operatorname{dexp}_{-\xi_i}$, the expression on the right hand side can be expanded as an infinite series in $\operatorname{ad}_{\omega_i^+(\boldsymbol{\xi})}$ and $\operatorname{ad}_{\xi_i}$ applied to $\delta\xi_i$. (Recall that the effect of π_{p_i} is to cancel out Lie monomials of even degree.) The crucial point is that there is a cancellation in the leading term so that, neglecting terms of fourth order and higher,

$$\begin{aligned}&\delta\xi_i - (\pi\circ\operatorname{dexp}_{-\omega_i^+(\boldsymbol{\xi})})^{-1}\circ(\pi\circ\operatorname{Ad}_{\exp(-\omega_i^+(\boldsymbol{\xi}))}\circ\operatorname{dexp}_{-\xi_i})(\delta\xi_i) = \\ &-\frac{1}{3}\operatorname{ad}^2_{\omega_i^+(\boldsymbol{\xi})}(\delta\xi_i) - \frac{1}{6}\operatorname{ad}^2_{\xi_i}(\delta\xi_i) - \frac{1}{2}\operatorname{ad}_{\omega_i^+(\boldsymbol{\xi})}\operatorname{ad}_{\xi_i}(\delta\xi_i) + \mathcal{O}(K^4\|\omega_i^+(\boldsymbol{\xi})\|^4\|\delta\xi_i\|, K^4\|\xi_i\|^4\|\delta\xi_i\|).\end{aligned}$$

We thus get

$$\frac{\partial\phi_i^+}{\partial\xi_i} = -\frac{1}{4}\left(\frac{1}{3}\operatorname{ad}^2_{\omega_i^+(\boldsymbol{\xi})} + \frac{1}{6}\operatorname{ad}^2_{\xi_i} + \frac{1}{2}\operatorname{ad}_{\omega_i^+(\boldsymbol{\xi})}\operatorname{ad}_{\xi_i} + \mathcal{O}(K^4\|\omega_i^+(\boldsymbol{\xi})\|, K^4\|\xi_i\|^4)\right)$$

The proposition follows by taking norms. □

It is also possible to bound the derivatives of the boundary condition functions:

Proposition C.6.

(i) *For clamped splines* $\frac{\partial\phi_0}{\partial\xi_1} = 0$, $\frac{\partial\phi_N}{\partial\xi_{N-1}} = 0$

(ii) *For natural splines*

$$\left\|\frac{\partial\phi_0}{\partial\xi_1}\right\| \leq \frac{1}{2} + \frac{1}{3}K^2\|\phi_0\|^2 + \frac{1}{12}K^2\|\xi_1\|^2 + \mathcal{O}(K^4\|\boldsymbol{\xi}\|^4)$$

Proof.

(i) For clamped splines, ϕ_0 and ϕ_N are constant
(ii) For natural splines, we have

$$\exp(2\phi_0(\boldsymbol{\xi}))\cdot p_0 = \exp(-\xi_1)\cdot p_1$$

Differentiating and taking norms, we get

$$2\|\pi_{p_0}\circ \operatorname{dexp}_{-2\phi_0}\delta\phi_0\| = \|\pi_{p_1}\circ\operatorname{dexp}_{\xi_1}\delta\xi_1\|$$

Lemma A.5 now gives

$$\|\delta\phi_0\| \leq \frac{1}{2}\frac{2K\|\phi_0\|}{\sin(2K\|\phi_0\|)}\frac{\sinh(K\|\xi_1\|)}{K\|\xi_1\|},$$

and the claim follows by a Taylor expansion of $\frac{x}{\sin(x)}$ and $\frac{\sinh(x)}{x}$.

□

C.3. **Convergence.** We are now ready to prove the convergence theorem.

Proof of Theorem 3.1. A consequence of Proposition C.1 is that ϕ has an invariant region for small enough D. We need to also establish that it is a contraction. It is sufficient to show that $\|\mathbf{T}\boldsymbol{\phi}\| \leq \alpha < 1$.

We have

$$\|\mathbf{T}\boldsymbol{\phi}\| = \max_{0\leq i\leq N}\|\mathbf{T}\phi_i\|$$

and

$$\begin{aligned}
\|\mathbf{T}\phi_0\| &= \left\|\frac{\partial\phi_0(\boldsymbol{\xi})}{\partial\xi_1}\right\| \\
\|\mathbf{T}\phi_i\| &= \left\|\frac{\partial\phi_i(\boldsymbol{\xi})}{\partial\xi_{i-1}}\right\| + \left\|\frac{\partial\phi_i(\boldsymbol{\xi})}{\partial\xi_i}\right\| + \left\|\frac{\partial\phi_i(\boldsymbol{\xi})}{\partial\xi_{i+1}}\right\| \\
\|\mathbf{T}\phi_N\| &= \left\|\frac{\partial\phi_N(\boldsymbol{\xi})}{\partial\xi_{N-1}}\right\|
\end{aligned}$$

By Proposition C.3, Proposition C.4, and Proposition C.6, we can bound the terms appearing with a Taylor expansion

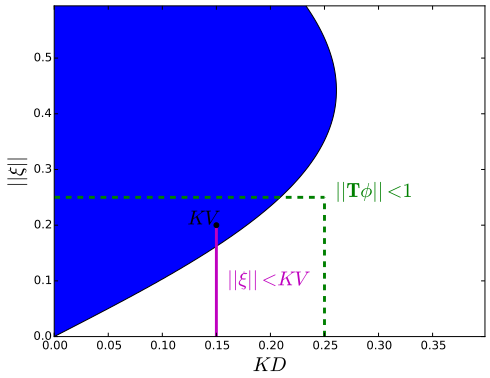

FIGURE 11. An illustration of the convergence argument. The blue area denotes the values (KD, KV) satisfying (40). The green dashed lines illustrate the condition $K\max(D, \|\boldsymbol{\xi}\|)$ sufficiently small. "Sufficiently small" is not quantified, and the lines are just an illustration. To ensure a solution, KV has to be in the blue area, and the magenta line has to be contained in the dashed green rectangle.

to obtain

$$\begin{aligned}
\|\mathbf{T}\phi_i\| \leq & \frac{1}{4}\left(1 + \frac{1}{6}K^2\|\omega_i^-(\boldsymbol{\xi})\|^2 + \frac{1}{6}K^2\|\xi_i\|^2\right) \\
& + \frac{1}{4}K^2\left(\frac{1}{3}\|\omega_i^-(\boldsymbol{\xi})\|^2 + \frac{1}{6}\|\xi_i\|^2 + \frac{1}{2}\|\xi_i\|\|\omega_i^-(\boldsymbol{\xi})\|\right) \\
& + \frac{1}{4}K^2\left(\frac{1}{3}\|\omega_i^+(\boldsymbol{\xi})\|^2 + \frac{1}{6}\|\xi_i\|^2 + \frac{1}{2}\|\xi_i\|\|\omega_i^+(\boldsymbol{\xi})\|\right) \\
& + \frac{1}{4}\left(1 + \frac{1}{6}K^2\|\omega_i^+(\boldsymbol{\xi})\|^2 + \frac{1}{6}K^2\|\xi_i\|^2\right) + \mathcal{O}(K^4\|\boldsymbol{\omega}\|^4, K^4\|\boldsymbol{\xi}\|^4) \\
\leq & \frac{1}{2} + \frac{1}{4}K^2\|\boldsymbol{\omega}\|^2 + \frac{1}{6}K^2\|\boldsymbol{\xi}\|^2 + \frac{1}{4}K^2\|\boldsymbol{\xi}\|\|\boldsymbol{\omega}\| + \mathcal{O}(K^4\|\boldsymbol{\omega}\|^4, K^4\|\boldsymbol{\xi}\|^4).
\end{aligned}$$

We can now use (39) and Proposition C.6 to obtain a bound of the form

$$\|\mathbf{T}\boldsymbol{\phi}\| \leq \frac{1}{2} + \mathcal{O}(K^2D^2, K^2\|\boldsymbol{\xi}\|^2).$$

It is therefore clear that when $K\max(D, \|\boldsymbol{\xi}\|)$ is sufficiently small, ϕ is a contraction. When D approaches zero, the smallest V satisfying (40) also approaches zero. Therefore, when D is small enough, there is a V such that

- $\{\boldsymbol{\xi} \mid \|\boldsymbol{\xi}\| \leq V\}$ is an invariant region and
- $\|\mathbf{T}\boldsymbol{\phi}\| \leq \alpha \leq 1$ on that region

Therefore, the fixed point iteration converges to a solution. □

See also Figure 11 for an illustration of the final argument.

Appendix D. Python implementation

Here we briefly indicate how to use our `Python` implementation to compute splines in various geometries. First, one has to install the following package by following the installation instructions:

https://github.com/olivierverdier/bsplinelab

The minimal necessary import is

```
from bspline.interpolation import Symmetric, cubic_spline
```

Here is an example of how to interpolate between random points in the Euclidean case:

```
# 10 random points in R^4:
interpolation_points = np.random.rand(10,4)
b = cubic_spline(Symmetric, interpolation_points)
```

The result is then a C^2 function `b` which is equal to the interpolation points at integer points on the interval $[0, 9]$.

In order to interpolate on, for instance, a sphere, one would do as follows:

```
from bspline.geometry import Sphere
# 3 points on the sphere:
interpolation_points = np.array([[1.,0,0], [0,1,0], [0,0,1]])
b = cubic_spline(Symmetric, interpolation_points, geometry=Sphere())
```

The function `b` is now a function defined on the interval $[0, 2]$ such that it is C^2, is interpolating the prescribed points at the integer points 0, 1 and 2, and is on the sphere for all points in between.

For further information on `bsplinelab`, we refer to the package documentation and the available code examples.

References

[1] D. C. Brody, D. D. Holm, and D. M. Meier, Quantum splines, *Phys. Rev. Lett.* **109** (2012), 100501.

[2] P. Crouch and F. S. Leite, Geometry and the dynamic interpolation problem, *American Control Conference, 1991*, pp. 1131–1136, IEEE, 1991.

[3] D. Dong and I. R. Petersen, Quantum control theory and applications: a survey, *IET Control Theory & Applications* **4** (2010), 2651–2671.

[4] S. Helgason, *Differential Geometry and Symmetric Spaces*, Pure and applied mathematics, American Mathematical Society, 1962.

[5] D. Kendall, D. Barden, T. Carne, and H. Le, *Shape and Shape Theory*, Wiley Series in Probability and Statistics, Wiley, 2009.

[6] T. W. B. Kibble, Relativistic models of nonlinear quantum mechanics, *Comm. Math. Phys.* **64** (1978), 73–82.

[7] T. W. B. Kibble, Geometrization of quantum mechanics, *Comm. Math. Phys.* **65** (1979), 189–201.

[8] K. A. Krakowski, L. Machado, F. Silva Leite, and J. Batista, A modified Casteljau algorithm to solve interpolation problems on Stiefel manifolds, *Journal of Computational and Applied Mathematics* **311** (2017), 84–99.

[9] J. M. Lee, *Riemannian manifolds*, vol. 176 of *Graduate Texts in Mathematics*, Springer-Verlag, New York, an introduction to curvature, 1997.
[10] H. Z. Munthe-Kaas and O. Verdier, Integrators on homogeneous spaces: Isotropy choice and connections, *Foundations of Computational Mathematics* **16** (2016), 899–939, 1402.6981.
[11] L. Noakes, Duality and Riemannian cubics, *Advances in Computational Mathematics* **25** (2006), 195–209.
[12] L. Noakes, G. Heinzinger, and B. Paden, Cubic splines on curved spaces, *IMA J. Math. Control Inform.* **6** (1989), 465–473.
[13] F. C. Park and B. Ravani, Bézier Curves on Riemannian Manifolds and Lie Groups with Kinematics Applications, *Journal of Mechanical Design* **117** (1995), 36.
[14] T. Popiel and L. Noakes, Bézier curves and C2 interpolation in Riemannian manifolds, *Journal of Approximation Theory* **148** (2007), 111–127.
[15] C. Samir, P.-A. Absil, A. Srivastava, and E. Klassen, A Gradient-Descent Method for Curve Fitting on Riemannian Manifolds, *Foundations of Computational Mathematics* **12** (2011), 49–73.
[16] R. Sharpe, *Differential geometry: Cartan's generalization of Klein's Erlangen program*, Graduate texts in mathematics, Springer, 1997.